Scanning tunnelling microscopy imaging and spectroscopy of p-type degenerate 4H-SiC(0001)

2005 J. Phys.: Condens. Matter 17 4015

(http://iopscience.iop.org/0953-8984/17/26/002)

INSTITUTE OF PHYSICS PUBLISHING JOURNAL OF PHYSICS: CONDENSED MATTER

J. Phys.: Condens. Matter **17** (2005) 4015–4022 doi:10.1088/0953-8984/17/26/002

Scanning tunnelling microscopy imaging and spectroscopy of p-type degenerate 4H-SiC(0001)

A Laikhtman, G Baffou, A J Mayne and G Dujardin

Laboratoire de Photophysique Moléculaire, CNRS, Bâtiment 210, Université Paris Sud, 91405 Orsay, France

Received 24 February 2005, in final form 17 May 2005
Published 17 June 2005
Online at stacks.iop.org/JPhysCM/17/4015

Abstract

In this work we present scanning tunnelling microscopy (STM) imaging and spectroscopy of a highly p-doped wide bandgap semiconducting 4H-SiC(0001) surface. Whereas n- and p-doped 6H-SiC or n-doped 4H-SiC surfaces can be relatively easily imaged with the STM, the p-doped 4H-SiC cannot be imaged due to the absence of any surface conductivity. This is very surprising given the presence of a p-doped, degenerate epitaxial layer. The behaviour can be explained by the formation of a Schottky barrier either between the tip and the surface or between the surface and the sample holder, depending on the polarity of the applied voltage. We found that prolonged and repeated exposures of the SiC surface to a Si atomic flux followed by thermal annealing are required before the surface conductivity is sufficient to allow STM images to be recorded. The result is the deposition of overlayers of Si, with structures similar to Si(111) 7×7, Si(113) 3×2, and Si(110) 16×2 rather than the expected stable SiC(0001) 3×3 reconstruction. We have further demonstrated the ability of scanning tunnelling spectroscopy to distinguish between the Si and the SiC phases based on the difference in their bandgaps.

1. Introduction

Surface imaging of semiconducting materials by scanning tunnelling microscopy (STM) is of great importance in understanding the performance of semiconductor based electronic devices due to the crucial role of surface morphology, structure, purity and electronic properties. It is only very recently that well defined SiC surfaces, understood at the atomic scale, could be obtained [1–11]. This has opened up the possibility of investigating the effect of adsorbate species such as molecules or metals on SiC surfaces and the corresponding interfaces [11–13]. While narrow bandgap materials (e.g. Si, Ge) can be easily studied, STM measurements of wide bandgap semiconductors seem to be much more difficult to obtain. Two aspects need to be highlighted. Firstly, there is little mention of the influence of the type of dopant and concentration on the ease of obtaining STM images. It is generally accepted that increasing

the dopant concentration should enable STM measurements to be performed, so that not much attention is paid to the type of the doping and the electronic structure of the studied samples. Indeed, the difficulties observed during such experiments are often attributed to problems related to tip and surface preparation. Most STM measurements have been performed for 6H-SiC (mostly n-doped) while very few data exist for 4H-SiC and only on n-doped samples [7, 9, 14]. Our study appears to be the first on a p-doped 4H-SiC surface. We found that the p-doped 4H-SiC surface cannot be imaged with the STM under normal conditions due to the absence of any surface conductivity. We will show that the surface conductivity can be sufficiently modified by depositing surplus silicon to enable STM imaging. Secondly, we would like to draw attention to the formation of Schottky barriers either between the tip and the surface or between the surface and the sample holder [15]. This is crucial as applications often require the use of a highly doped, even degenerate material, while still maintaining such important properties as optical transparency, high thermal conductivity, and surface chemical stability. Consequently, their electrical conductivity is vital. Depending on the polarity of the applied voltage the formation of Schottky barriers prevents STM imaging of even very highly doped semiconducting surfaces. The tunnelling current cannot pass at low bias voltages either from the semiconductor to the tip, at negative bias, or from the semiconductor surface to the substrate holder, at positive voltage.

STM measurements are still essential due to the constantly growing use of wide bandgap materials such as diamond, diamond-like carbon, and silicon carbide (SiC) in high temperature, high power, high frequency, and high voltage electronic devices and sensors [1–4]. Despite a higher carrier mobility for the cubic β-SiC, the hexagonal 6H- and 4H-SiC phases are currently utilized for potential applications, primarily because of the availability of much better quality single-crystal wafers, but also because of their wider energy bandgaps. The bandgap of 6H- and 4H-SiC ranges from 3.0 eV (6H) to 3.4 eV (4H) as compared to 2.4 eV for the 3C-SiC.

In this paper, we will discuss the results of our attempts to overcome the absence of surface conductivity through the deposition of a surplus of silicon and show that scanning tunnelling spectroscopy (STS) measurements give helpful insight into the surface conductivity.

2. Experimental details

SiC exists in cubic (3C), hexagonal (6H, 4H, 2H), and rhombohedric (15R) crystallographic phases amongst the 170 polytypes. Due to the rather recent availability of large enough wafers, 6H- and 4H-SiC polytypes are at present the most commonly used in SiC device applications [15]. Our experiments were performed at room temperature using an Omicron STM operating at pressures below 5×10^{-11} Torr. The sample used was a thyristor-type, single-crystal SiC wafer composed of an n-doped (nitrogen) 4H-SiC(0001) substrate covered by four differently doped layers (from the bulk towards the surface, namely n- (1.4×10^{19} cm^{-3}), p- (2.6×10^{15} cm^{-3}), n- (9.1×10^{17} cm^{-3}), and p-doped (1.0×10^{19} cm^{-3}) layers of the thickness of 0.5, 2.0, 0.3, and 0.2 μm, respectively. The last or top-most layer has degenerate characteristics. p-type doping was produced by introduction of aluminium acceptors. The sample was supplied by CREE-Research Co, and was the only degenerate p-doped 4H-SiC sample available at that time.

The preparation procedure for the hexagonal SiC surface had been developed earlier for the n-doped 6H-SiC [16] and was applied in this work. It includes the following steps: (i) the surface is flashed several times at 1100 °C to remove the native oxide; (ii) it is annealed between 1000 and 650 °C; (iii) to compensate for Si atoms lost during annealing, Si is deposited during a 15 min evaporation using a Si wafer resistively heated to 1150 °C and placed 15 mm from the hot sample (heated simultaneously to 650 °C); (iv) a series of 5 min thermal annealing

processes from 850 °C down to 650 °C; and (v) a slow cooling down (<50 °C min^{-1}) to room temperature. The surface quality was regularly checked by low energy electron diffraction (LEED) with the aim of obtaining the highly stable 3×3 reconstruction [8, 16, 17]. In contrast to the 6H-SiC, the LEED pattern of the 4H-SiC surface was of reasonable quality only after two or three cycles of Si deposition/SiC annealing.

3. Results and discussion

The first problem encountered while working with the SiC wafer is related to sample annealing during surface preparation. By using a degenerate semiconducting sample we expected to easily heat it resistively. However, the temperature response was very slow at low voltages and comparable to insulators: higher voltages were required to initiate heating. Two effects can contribute to the problem of sample heating. The first one is related to the thyristor configuration of the SiC wafer. Thyristors have an intermediate layer with a very low dopant concentration, 2.6×10^{15} cm^{-3} in our case, which blocks the current transfer through the sample at low voltages. However, the current could still pass through the highly doped layers close to the surface, albeit restricted by the thinness of the layer. This is why we have considered the electronic band structure of p-doped SiC including the contact with a Mo substrate holder, as shown in figure 1. The system is characterized by the following parameters: the Fermi level position coincides with the valence band maximum (degenerate sample) or is very close to it; the electron affinity X of 4H-SiC is ∼2.2 eV; the energy bands in the semiconductor are bent strongly downward by ∼1.7 eV, but the bending region is very narrow due to the high concentration of dopants [15]; the work function of p-doped SiC is significantly higher than that of Mo, producing a Schottky barrier. In a p-doped semiconductor the majority carriers are holes, which, in our case, cannot contribute to the current due to the lack of majority carriers in the band-bending region, so no ohmic contacts are produced. Hence, at low voltages no or very little current passes through the sample, and consequently resistive heating of the SiC material is difficult.

Another effect which substantially hindered obtaining STM images even after a few cycles of surface preparation was the absence of the tunnelling current at bias voltages between −5 and +5 V. To explain the problem concerning the tunnelling current, a second metallic surface is added to the model (which represents an STM tip made from tungsten) on the opposite side of the sample separated by a narrow vacuum region through which tunnelling takes place. The modified scheme is shown in figure 1(b). Since the work functions of W and Mo are nearly identical, 4.55 and 4.60 eV, respectively, the band structure obtained at zero bias voltage is symmetric. When applying a small negative bias potential, for example −2 V, to the sample (i.e., the Fermi level of the W tip is lower by 2 V than that of the sample and Mo), the band bending on the tungsten side increases, as shown in figure 1(c). It is clear from this figure that current could now pass from Mo to SiC but it still cannot pass from SiC to the tip. The same effect occurs at low positive voltages but the passage of the current is blocked in the opposite direction. When decreasing a bias potential to, for example, −5 V, the band bending on the tip side increases further and the passage of the carriers is still blocked.

A LEED pattern (not shown) of the surface, prepared as explained above, was obtained by irradiating the sample by an electron beam having an incident energy of 93 eV. A 3×3 surface reconstruction was observed. There is no evidence of the $6\sqrt{3} \times 6\sqrt{3}$ surface reconstruction although some studies suggest that the preparation conditions applied here should favour its formation [14, 18, 19]. We cannot exclude, however, some traces of the $\sqrt{3} \times \sqrt{3}$ reconstruction, which is also typical of these prepared 4H-SiC surfaces [19, 20]. There are a few spots not related to either the $\sqrt{3} \times \sqrt{3}$ or the 3×3 reconstructions: their origin has not yet been identified.

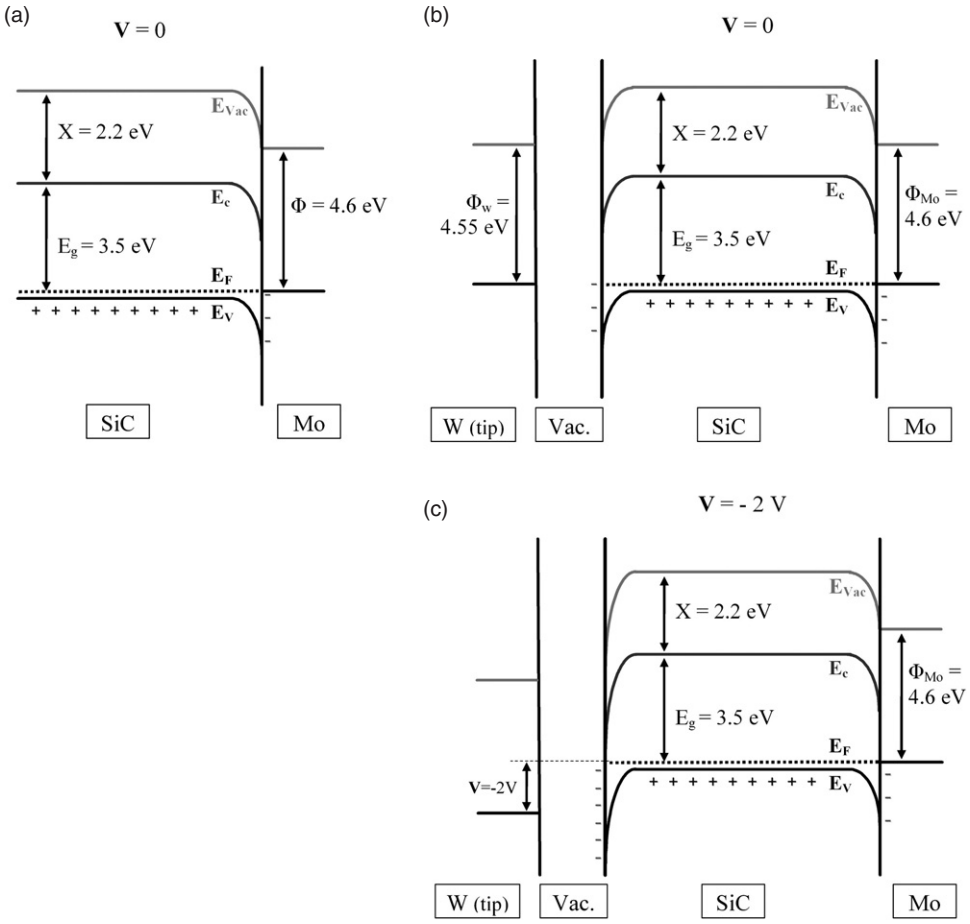

Figure 1. Schematic diagrams of the electronic band structure of the p-doped 4H-SiC surface (a) in contact with a Mo substrate holder, (b) in contact with a Mo substrate holder and a tungsten STM tip (separated from the SiC and Mo by a tunnelling vacuum region) at zero bias voltage; (c) in contact with a Mo substrate holder and a tungsten STM tip at a bias potential of −2 V.

After a number of surface preparation cycles, namely Si deposition/sample annealing of 4H-SiC, we succeeded in recording STM images. These are shown in figure 2 and described below. In figure 2(a) an STM image obtained after several cycles of Si deposition/annealing is shown. The image was recorded with a sample bias of −4.0 V at 0.5 nA. As has just been mentioned, the LEED pattern of the surface displayed a less than perfect 3 × 3 reconstruction. The STM image shows a pseudo-cubic surface reconstruction with a repeat distance corresponding to a 3 × 2 structure. The appearance is very similar to that of the previously observed 3 × 2 on Si(113) [21]. However, the local atomic structure may or may not be the same. We can only conjecture on what we see: bright lines with side spots at regular intervals with the spots only on one side of the line. The lines could be π-chains as for the cleaved Si(111)-2 × 1 surface. On the other hand they could be tetramers (tetrahedra) similar to the SiC 3 × 3 surface, as the triangles that can be discerned between the ordered domains could correspond to a trimer base. The structure is quite different, however, from the dimer-row structure of the 3 × 2 reconstructed surface of β-SiC(100) [5, 6].

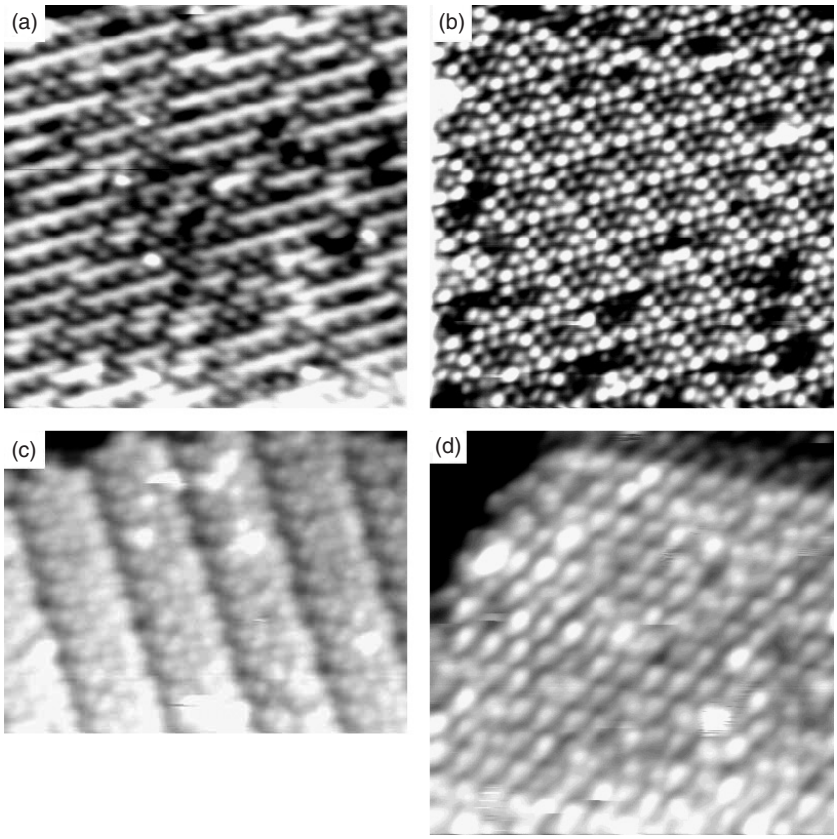

Figure 2. (a) A 20 nm × 20 nm STM image (−4.0 V, 0.5 nA) of the surface reconstructed similar to Si(113) 3 × 2. (b) A 20 nm × 20 nm STM image (−1.5 V, 0.3 nA) of the surface reconstructed similar to Si(100) 7 × 7. (c) A 10 nm × 15 nm STM image (−4 V, 0.3 nA) of the surface having a structure resembling that of Si(110) 16 × 2. (d) A 20 nm × 20 nm STM image (−4 V, 0.5 nA) of the hexagonal structure observed only locally on the 4H-SiC surface.

An STM image shown in figure 2(b) and recorded at a sample bias of −1.5 V and tunnelling current of 0.3 nA displays another type of surface geometry. This surface was obtained after a large number of Si deposition/SiC annealing cycles. One can observe a reconstruction similar to that of the 7 × 7 for Si(111), although the dimensions of the unit cell are slightly different: 29 Å compared to the literature value of 26.9 Å for Si(111). The structure seems quite clear from the STM images. The difference between the unit cell values may be due either to the piezo calibration (the uncertainty is of the order of 10%) or to the size mismatch between the crystalline structure of Si and SiC.

In figure 2(c) we show an STM micrograph recorded at −4 V and 0.3 nA after the surface had been prepared under conditions similar to those of figure 2(a). There are bright chains running parallel to each other separated by a distance of 50 Å. This type of structure resembles that of the Si(110) 16 × 2 reconstructed surface [22, 23]. Again, the real structure is not known, but the fact that the detail within each terrace and on different terraces is the same suggests that we are seeing a local ordered structure on the surface with a repeat distance corresponding roughly to a 16 × 2. The images with the 3 × 2, 7 × 7, and 16 × 2-like structures were generally recorded after a number of Si deposition cycles and also all three structures were observed

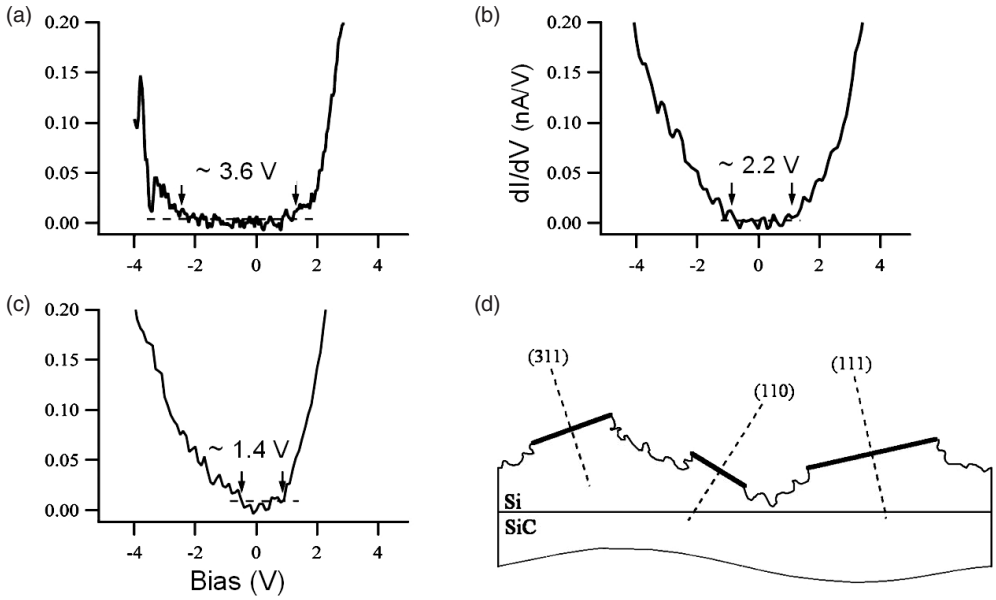

Figure 3. STS derivative, $\mathrm{d}I/\mathrm{d}V$ as a function of bias (V), curves measured on the different reconstructed surfaces when optimal imaging conditions could be obtained: (a) hexagonal 3×3 reconstructed 4H-SiC surface; (b) the apparent Si(113) 3×2 reconstruction on the 4H-SiC surface; (c) the apparent Si(110) 16×2 surface structure on the 4H-SiC surface. (d) A schematic diagram of the possible geometry of the SiC surface following prolonged deposition of Si.

on the *same* sample. This clearly indicates the existence of regions where the deposition of a surplus of silicon has occurred.

Finally, in the STM image (−4 V, 0.5 nA) shown in figure 2(d) one can see a hexagonal atomic arrangement. We had expected to see this surface regularly; however, it was seen only occasionally. The local structure in the STM image corresponds to a 4×4 pattern.

In figure 3 we present STS ($\mathrm{d}I/\mathrm{d}V$ as a function of bias voltage) derivative curves measured when optimal imaging conditions were obtained. These curves were recorded for most of the discussed surface structures. In all the curves there is a certain zero-current region representing the bandgap of the respective surface. We would like to note that STS curves measured after a small number of Si deposition/annealing cycles (not shown) generally had a very wide zero-current region, initially greater than 8 V, which is of course not the true bandgap of the studied material. After repeated surface preparation cycles the gap gradually diminished to these final ranges. Curve (a) was measured for the hexagonal surface and one can observe a zero-current region ranging from −2 to +1.5 V which is in good agreement with the 4H-SiC bandgap of 3.4 eV. Curves (b) and (c) were measured on the surfaces with the reconstructions similar to Si(113) 3×2 and Si(110) 16×2, respectively. Their bandgaps are reduced to ∼1.7 V; this is close to the bandgap of Si, which could corroborate the deposition of a surplus of silicon.

Hexagonal atomic arrangements were observed only in very localized regions, while the STM shows mostly dimer-like structures. Similar features were previously observed on Si(113) [21], and, to some extent, under Si rich conditions, on 6H-SiC [24]. In our case, we had repeatedly exposed the SiC surface to a Si flux to obtain a surface with electrical and electronic properties suitable for STM measurements. If we look carefully at the LEED pattern, the additional spots do not appear to belong to the 3×3 reconstruction; instead, we

may attribute them to the 3×2 reconstructed areas. This assumption is supported by the fact that the 3×3 reconstruction was less pronounced in the LEED pattern when measured at lower, more surface sensitive incident electron energy, 46 eV (not shown). It is not evident that a 3×2 'cubic' reconstruction should be formed on a hexagonal surface. Also our STM images differ significantly from those observed on the 3×2 reconstructed cubic SiC surface [7]. However, this is not the first time that a 'cubic' pattern has been observed on a hexagonal surface: a 4×3 structure has been obtained on the 6H-SiC [16] and a 3×2 pattern was reported before for the $\sqrt{3} \times \sqrt{3}$ reconstructed 6H-SiC surface [24]. The same work [24] shows that the Si(111) 7×7 structure may be grown on the $\sqrt{3} \times \sqrt{3}$ SiC surface under the conditions similar to those applied here. Likewise, Kulakov *et al* [17] observed that, on the 6H-SiC(0001)-3×3 surface, surplus silicon aggregated into large islands on which the 7×7 reconstruction could be seen.

The presence of these different surface reconstructions, more characteristic of Si than SiC, indicates that prolonged and repeated exposure to Si vapour results in the formation of facetted Si structures reconstructed in at least three different ways, as schematically presented in figure 3(d). These facets are surrounded by unreconstructed zones which are difficult to image in STM.

4. Conclusion

In summary, we have proposed an explanation as to the difficulty of recording STM images on the as-prepared p-doped degenerate 4H-SiC surface. The problem originates from the combined electronic band structure of the tip–SiC–sample holder system which prevents the passage of the tunnelling current at reasonable bias voltages, both positive and negative.

The preparation procedure had been successfully tested previously for n-doped 6H-SiC [11], and in that case produced mostly the 3×3 reconstructed surface, as identified by STM and LEED. However, when applied here to the 4H-SiC surface, a number of cycles of surface preparation, in particular Si deposition followed by sample annealing, were necessary to record STM images of reasonable quality. Despite an apparent 3×3 LEED pattern, a number of STM images measured in this work were found to be identical to that of Si(111) 7×7. The STM images showed additional structures resembling the Si(113) 3×2 and the Si(110) 16×2 surfaces. These are due to the over-deposition of a few atomic layers of Si, which enable the tunnelling current to pass by reducing the bandgap.

Although the surplus Si atoms are arranged in a few atomic layers, as is evident from LEED, STS spectroscopy is capable of differentiating between the SiC and the Si phases based on the difference in their bandgaps.

Acknowledgments

This work has been undertaken as part of an EU funded STREP 'Nanoman' (contract NMP4-CT-2003-550660) and the European RTN network 'AMMIST' (contract HPRN-CT-2002-02999).

References

[1] Doğan S, Teke A, Huang D, Morcoç H, Roberts C B, Parish J, Ganguly B, Smith M, Myers R E and Saddow S E 2003 *Appl. Phys. Lett.* **82** 3107
[2] Ramachandran V and Feenstra R M 1999 *Phys. Rev. Lett.* **82** 1000
[3] Alok D, Egloff R and Arnold E 1998 *Mater. Sci. Forum* **264** 929
[4] Choyke W J, Matsunami H M and Pensl G (ed) 1998 *Silicon Carbide, A Review of Fundamental Questions and Applications to Current Device Technology* vol 1 and 2 (Berlin: Akademie-Verlag)

[5] Soukiassian P 2002 *Mater. Sci. Forum* **389** 691
[6] Semond F, Soukiassian P, Mayne A J, Dujardin G, Douillard L and Jaussaud C 1997 *Phys. Rev. Lett.* **77** 2013
[7] Starke U, Schardt J, Bernhardt J, Franke M and Heinz K 1999 *Phys. Rev. Lett.* **82** 2107
[8] Bernhardt J, Nerding M, Starke U and Heinz K 1999 *Mater. Sci. Eng.* B **61** 207
[9] Wagner G, Doerschel J and Gerlitzke A 2001 *Appl. Surf. Sci.* **184** 55
[10] Starke U, Bernhardt J, Franke M, Schardt J and Heinz K 1997 *Diamond Relat. Mater.* **6** 1349
[11] Amy F, Enriquez H, Soukiassian P, Storino P-F, Chabal Y J, Mayne A J, Dujardin G, Hwu Y K and Brylinski C 2001 *Phys. Rev. Lett.* **86** 4342
[12] Derycke V, Pham N P, Fonteneau P, Soukiassian P, Aboulet-Nze P, Monteil Y, Mayne A J, Dujardin G and Gautier J 2000 *Appl. Surf. Sci.* **162** 413
[13] Iwami M, Hirai M, Kusaka M, Mihara I, Saito T, Yamaguchi M, Morii T and Watanabe M 2000 *Mater. Sci. Forum* **338** 419
[14] Starke U, Schardt J and Franke M 1997 *Appl. Phys.* A **65** 587
[15] Mathieu H 2001 *Physique des Semiconducteurs et des Composants Métalliques* (Paris: Dunod) p 271 and 704
[16] Amy F, Enriquez H, Soukiassian P, Brylinski C, Mayne A J and Dujardin G 2001 *Appl. Phys. Lett.* **79** 767
[17] Kulakov M A, Henn G and Bullemer B 1996 *Surf. Sci.* **346** 49
[18] Schardt J, Bernhardt J, Starke U and Heinz K 2000 *Phys. Rev.* B **62** 10335
[19] Tsukamoto T, Hirai M, Kusaka M, Iwami M, Ozawa T, Nagamura T and Nakata T 1997 *Surf. Sci.* **371** 316
[20] Diani M, Diouri J, Kubler L, Simon L, Aubel D and Bolmont D 2003 *Surf. Rev. Lett.* **10** 55
[21] Knall J, Pethica J B, Todd J D and Wilson J H 1991 *Phys. Rev. Lett.* **66** 1733
[22] An T, Yoshimura M, Ono I and Ueda K 2000 *Phys. Rev.* B **61** 3006
[23] Yamamoto Y 1994 *Phys. Rev.* B **50** 8534
[24] Li L, Hasegawa Y, Sakurai T and Tsong I S T 1996 *J. Appl. Phys.* **80** 2524